

Figure 5

Induction of apoptotic T98G cells *in vitro* by overexpression of HCOL1A1. Mock cells (Mock) and HCOL1A1-transfected cells (HCOL1A1-I and HCOL1A1-II) were assayed for apoptosis using the *in situ* TUNEL method. (a) The photomicrographs of Apoptotic cells. Magnification, $\times 200$. (b) The percentage of apoptotic cells represents the mean \pm SD (n = 5, duplicate experiment). *, $P < 0.001$, when tested against the Mock.

tumorigenesis, migration, proliferation, apoptosis, and morphogenesis, which are distinct from those of original intact molecules [2-11,32-36]. Endostatin, which is an NC1 fragment of type XVIII collagen, has been extensively studied in the angiogenesis field [4,37,38]. It has been reported that endostatin inhibits tumor cell invasion, as well as HCOL1A1 peptides, which were presented here. Endostatin inhibits tumor cell invasion by blocking the activation of latent matrix metalloprotease-2, -9, and -13 [39-41]. However, in this study, there was no difference in the level of activated MMP-2 and MMP-9 between HCOL1A1-transfected cells and Mock cells by gelatin zymography analysis (data not shown). This finding suggests that the HCOL1A1 peptide may have a unique function as a suppressor of tumor cell invasion that is distinct from that of NC1 fragments of basement membrane collagens. It was demonstrated that endostatin suppresses

cell proliferation *in vitro* and inhibits the growth of primary tumors and metastases by induction of apoptosis [42-44]. Similarly, the expression of HCOL1A1 peptides caused inhibition of tumor cell growth *in vitro* and complete regression of tumors in nude mice. Moreover, HCOL1A1 peptides induced apoptosis in glioma cells. Thus, HCOL1A1 peptides, as well as endostatin and other NC1 fragments of collagens, should also have a potential for anti-tumorigenesis. Interestingly, type I collagen is a fibrillar collagen, whereas fragments of collagens, which have so far been reported to inhibit tumor progression, are derived from basement membrane collagens. The HCOL1A1 peptides, which are derived from fibrillar collagen, may be novel inhibitors of tumor growth and invasion. In this report, the mechanism for the suppression of malignancy of T98G glioma is not evident, but it should become clear with further study.

Recently, significant technical advances in the treatment of gliomas have emerged, and gene therapy, in particular, is noted as a potent therapeutic strategy. The major approaches of gene therapy to glioma are based on apoptosis-related gene therapy [45], antiangiogenesis therapy [46,47], and immunotherapy [48,49]. Several ECM components and their fragments, such as decorin [20,30,31] and endostatin [46,50-54] are being tried as potential targets for glioma gene therapy. The HCOL1A1 gene may also be a good candidate as gene medicine for a novel therapy against glioma.

Conclusion

In summary, the tumor growth and invasion of malignant human gliomas were markedly suppressed by the introduction of HCOL1A1. The suppression of a malignant phenotype of glioma cells by HCOL1A1 provides the basis of a novel therapeutic approach.

Materials and methods

Cell culture

The human glioma T98G cells were derived from glioblastoma and obtained from the American Type Culture Collection. Cells were maintained and passaged in a minimum essential medium (MEM) supplemented with 10% fetal bovine serum (FBS), 1% nonessential amino acids, and 1 mM sodium pyruvate at 37°C.

HCOL1A1 expression plasmid

An $\alpha 1$ chain of the human type I procollagen expression vector, pCXN2/HCOL1A1, was constructed as follows. The cDNA of HCOL1A1 was cloned from a human heart cDNA library, and a partial cDNA fragment was synthesized by RT-PCR using mRNA of a normal human skin fibroblast. cDNA encoding the full-length HCOL1A1 gene was assembled from these fragments. The full-length HCOL1A1 cDNA was cloned into the downstream of the CAG promoter of a pCXN2 expression vector containing the neomycin resistance gene.

Cell transfection

Cells were transfected with pCXN2/HCOL1A1 or pCXN2 without an insert, as a Mock, by using LipofectAMINE 2000 (Invitrogen Corporation, CA) according to the manufacturer's protocol. Cells were selected in a medium containing 0.8 mg/ml of G418. G418-resistant colonies were cloned and expanded.

Immunocytochemical staining

T98G cells (1×10^5) were grown for 2 to 4 days on 6-cm culture dishes and fixed with cold methanol at -20°C for 5 min. The cells were permeated with 0.02% Triton X-100 in PBS for 15 min and pretreated with 3% H₂O₂ in methanol for 15 min to quench endogenous peroxidase activity. The cells were blocked with Block Ace (Dainippon

Pharmaceutical Co., Ltd., Osaka, Japan) overnight at 4°C and incubated with polyclonal anti- $\alpha 1(I)$ collagen antibody (L-19) (1:60) (Santa Cruz Biotechnology, Inc., CA) at 37°C for 1 h. Bound primary antibodies were labeled with biotinylated IgG antibodies (1:500) (Santa Cruz Biotechnology, Inc., CA) at 37°C for 15 min and incubated with streptavidin-peroxidase at 37°C for 20 min. HCOL1A1 peptides were visualized with diaminobenzidine, and nuclei were counterstained with hematoxylin.

In vitro growth assay

Individual clones were seeded in 96-well plates at a density of 5×10^2 cells per well in 100 μ l of a culture medium. At each time point, the cells were assayed for proliferation with TetraColor One, a cell-proliferation assay reagent (Seikagaku Co., Tokyo, Japan), according to the recommended method; they were then measured for absorbency at the well at 450 nm with a reference wavelength at 650 nm.

In vitro invasion and motility assay

In vitro invasion assays were performed using a Matrigel invasion chamber (8- μ m pore size, Becton Dickinson, Bedford, MA). A suspension of 2.5×10^4 cells in 0.5 ml of a serum free medium, Cosmedium 001, was added to the Matrigel chamber. The chambers were incubated at 37°C for 24 h in a 95% air/5% CO₂ incubator. The cells on the lower surface of the membrane were stained with Diff-Quik stain (Kokusaiyaku, Kobe, Japan). The invading cells were photographed under a microscope at $\times 100$ magnification and counted in five fields of four membranes.

A cell motility assay was performed in a similar manner except that the 8- μ m pore size PET membrane was not coated with Matrigel.

Tumor invasion into a matrigel wafer

The reconstituted basement membrane wafers were made by adding 1 ml of Growth Factor Reduced Matrigel (Becton Dickinson, MA) to a well of a 24-well plate and gelled at 37°C for 30 min. 1×10^5 cells were plated onto the surface of each wafer. On days 3 and 7 after plating, Matrigel wafers and adherent cells were fixed with 4% paraformaldehyde in PBS for 1 h. The wafers were then dehydrated through a graded ethanol series and embedded in paraffin. Sections were cut and stained with hematoxylin and eosin.

In vivo tumor formation

T98G cells (4.3×10^6) were implanted subcutaneously in 100 μ l of a 1:1 mixture of a culture medium and Growth Factor Reduced Matrigel in the forelegs of the nude mice according to the method described by Rubenstein *et al.* [55] and Teicher *et al.* [56]. The tumor volume was meas-

ured with a caliper and calculated using the formula $\text{width}^2 \times \text{length} \times 0.5$. Animal experiments in the present study were performed in compliance with the guidelines of the Institute for Laboratory Animal Research, National Cancer Center Research Institute.

Apoptosis assay

In the normal growth medium, 1.8×10^5 cells were seeded onto 6-cm culture dishes. After 24 h, the cells were rinsed and cultured in a serum-free medium, Cosmedium 001, which contained no protein except insulin and transferrin and was supplemented with sodium ascorbate (50 $\mu\text{g}/\text{ml}$) to avoid the effects of several ECM proteins carried by the serum. Five days later, the cells were assayed for apoptosis by the TUNEL method with the *In Situ* Cell Death Detection Kit, POD (Roche, Switzerland) according to the manufacturer's instructions. Apoptotic cells were identified by diaminobenzidine staining, and nuclei were counterstained with hematoxylin. The number of apoptotic cells was counted in five microscopic fields.

Statistical analysis

The results are given as means \pm SD. Student's t-test was performed for statistical evaluation, with $P < 0.05$ considered significant.

Abbreviations

ECM, extracellular matrix; HCOLIA1, human collagen type I $\alpha 1$.

Authors' contributions

KH carried out most of experiments. KH, TM and TO participated in its design and helped to the draft the manuscript. All authors read and approved the final manuscript.

Acknowledgements

We are grateful to Dr Masaaki Terada and Dr Hisae Hori for their participation in helpful discussions and to Dr Junichi Miyazaki of Osaka University, Osaka, Japan, for the kind gift of the CAG promoter. We also thank Ms Masako Hosoda, Mr Jun Onodera and Mr Kazuki Nemoto for their excellent technical work. This work was supported in part by Grants-in-Aid for the Second- and Third-Term Comprehensive 10-Year Strategy for Cancer Control, Health Science Research Grants for the Research on the Human Genome and Gene Therapy from the Ministry of Health, Labour and Welfare of Japan, a Grant-in-aid for Scientific Research on Priority Areas of the Ministry of Education, Culture, Sports, Science and Technology.

References

- Akamatsu H, Ichihara-Tanaka K, Ozono K, Kamikawa W, Matsuda H, Sekiguchi K: Suppression of transformed phenotypes of human fibrosarcoma cells by overexpression of recombinant fibronectin. *Cancer Res* 1996, **56**:4541-4546.
- Ortega N, Werb Z: New functional roles for non-collagenous domains of basement membrane collagens. *J Cell Sci* 2002, **115**:4201-4204.
- Clamp AR, Jayson GC: The clinical potential of antiangiogenic fragments of extracellular matrix proteins. *Br J Cancer* 2005, **93**:967-972.
- O'Reilly MS, Boehm T, Shing Y, Fukai N, Vasios G, Lane WS, Flynn E, Birkhead JR, Olsen BR, Folkman J: Endostatin: an endogenous inhibitor of angiogenesis and tumor growth. *Cell* 1997, **88**:277-285.
- Ramchandran R, Dhanabal M, Volk R, Waterman MJF, Segal M, Lu H, Knebelmann B, Sukhatme VP: Antiangiogenic activity of restin, NC10 domain of human collagen XV: comparison to endostatin. *Biochem Biophys Res Commun* 1999, **255**:735-739.
- Sasaki T, Larsson H, Tsi D, Claesson-Welsh L, Hohenester E, Timpl R: Endostatins derived from collagens XV and XVIII differ in structural and binding properties, tissue distribution and anti-angiogenic activity. *J Mol Biol* 2000, **301**:1179-1190.
- Colorado PC, Torre A, Kamphaus G, Maeshima Y, Hopfer H, Takahashi K, Volk R, Zamborsky ED, Herman S, Sarkar PK: Anti-angiogenic cues from vascular basement membrane collagen. *Cancer Res* 2000, **60**:2520-2526.
- Kamphaus GD, Colorado PC, Panka DJ, Hopfer H, Ramchandran R, Torre A, Maeshima Y, Mier JW, Sukhatme VP, Kalluri R: Constatin, a novel matrix-derived inhibitor of angiogenesis and tumor growth. *J Biol Chem* 2000, **275**:1209-1215.
- Maeshima Y, Manfredi M, Reimer C, Hothaus KA, Hopfer H, Chandamuri BR, Kharbada S, Kalluri R: Identification of the anti-angiogenic site within vascular basement membrane-derived tumstatin. *J Biol Chem* 2001, **276**:15240-15248.
- Hamano Y, Kalluri R: Tumstatin, the NC1 domain of alpha3 chain of type IV collagen, is an endogenous inhibitor of pathological angiogenesis and suppresses tumor growth. *Biochem Biophys Res Commun* 2005, **333**:292-298.
- Lima E, Silva R, Kachi S, Akiyama H, Shen J, Aslam S, Yuan Gong Y, Khu NH, Hatara MC, Boutaud A, Peterson R, Campochiaro PA: Recombinant non-collagenous domain of alpha2(IV) collagen causes involution of choroidal neovascularization by inducing apoptosis. *J Cell Physiol* 2006, **208**:161-166.
- Adams S, Sobel ME, Howard B, Olden K, Yamada KM, de Crombrughe B, Pastan I: Levels of translatable mRNAs for cell surface protein, collagen precursors, and two membrane proteins are altered in Rous sarcoma virus-transformed chick embryo fibroblasts. *Proc Natl Acad Sci USA* 1977, **74**:3399-3403.
- Sandmeyer S, Bornstein P: Declining procollagen mRNA sequence in chick embryo fibroblast infected with Rous sarcoma virus. *J Biol Chem* 1979, **254**:4950-4953.
- Vaheri A, Kirkinen M, Lehto VP, Linder E, Timpl R: Codistribution of pericellular matrix proteins in cultured fibroblasts and loss of transformation: fibronectin and procollagen. *Proc Natl Acad Sci USA* 1976, **75**:4944-4948.
- Tannapfel A, Anhalt K, Hausermann P, Sommerer F, Benicke M, Uhlmann D, Wittigmann H, Hauss J, Wittkind C: Identification of novel proteins associated with hepatocellular carcinomas using protein microarrays. *J Pathol* 2003, **201**:238-249.
- DeClerck YA, Bomann ET, Spengler BA, Biedler JL: Differential collagen biosynthesis by human neuroblastoma cell variants. *Cancer Res* 1987, **47**:6505-6510.
- Rutka JT, Giblin JR, Apodaca G, DeArmond SJ, Stern R, Rosenblum ML: Inhibition of growth and induction of differentiation in a malignant human glioma cell line by normal leptomeningeal extracellular matrix proteins. *Cancer Res* 1987, **47**:3515-3522.
- Savara J N, Wu C, Landy H, Wangpaljit M, Wei Y, Kuo MT, Robles C, Furst AJ, Tampidis T, Feun L: Procollagen alpha 1 type I: a potential aide in histopathological grading of glioma. *Cancer Invest* 2005, **23**:577-581.
- Tysnes BB, Mahesparan R: Biological mechanisms of glioma invasion and potential therapeutic targets. *J Neurooncol* 2001, **53**:129-147.
- Stander M, Naumann U, Dumitrescu L, Heneka M, Loschmann P, Gulbins E, Dichgans J, Weller M: Decorin gene transfer-mediated suppression of TGF-beta synthesis abrogates experimental malignant glioma growth in vivo. *Gene Ther* 1998, **5**:1187-1194.
- Bouterfa H, Darlapp AR, Klein E, Pletsch T, Roosen K, Tonn JC: Expression of different extracellular matrix components in human brain tumor and melanoma cells in respect to variant culture conditions. *J Neurooncol* 1999, **44**:23-33.
- Mahesparan R, Read TA, Lund-Johansen M, Skafnasmo KO, Bjerkvig R, Engebraaten O: Expression of extracellular matrix components in a highly infiltrative in vivo glioma model. *Acta Neuropathol (Berl)* 2003, **105**:49-57.

23. Khazenzon NM, Ljubimov AV, Lakhter AJ, Fujita M, Fujiwara H, Sekiguchi K, Sorokin LM, Petajaniemi N, Virtanen I, Black KL, Ljubimova JY: Antisense inhibition of laminin-8 expression reduces invasion of human gliomas *in vitro*. *Mol Cancer Ther* 2003, 2:985-994.
24. Hikawa T, Mori T, Abe T, Hori S: The ability in adhesion and invasion of drug-resistant human glioma cells. *J Exp Clin Cancer Res* 2000, 19:357-362.
25. Tew DS: Adhesive and invasive features in gliomas. *Pathol Res Pract* 2000, 196:701-711.
26. Utsuki S, Sato Y, Oka H, Tsuchiya B, Suzuki S, Fujii K: Relationship between the expression of E-, N-cadherin and beta-catenin and tumor grade in astrocytomas. *J Neurooncol* 2002, 57:187-192.
27. Asano K, Kubo O, Tajika Y, Huang MC, Takakura K, Ebina K, Suzuki S: Expression and role of cadherins in astrocytic tumors. *Brain Tumor Pathol* 1997, 14:27-33.
28. Shinoura N, Paradies NE, Warnick RE, Chen H, Larson JJ, Tew JJ, Simon M, Lynch RA, Kanai Y, Hirohashi S: Expression of N-cadherin and alpha-catenin in astrocytomas and glioblastomas. *Br J Cancer* 1995, 72:627-33.
29. Asano K, Duntsch CD, Zhou Q, Weimar JD, Bordelon D, Robertson JH, Pourmotabbed T: Correlation of N-cadherin expression in high grade gliomas with tissue invasion. *J Neurooncol* 2004, 70:3-15.
30. Munz C, Naumann U, Grimmec C, Rammensee HG, Weller M: TGF-beta-independent induction of immunogenicity by decorin gene transfer in human malignant glioma cells. *Eur J Immunol* 1999, 29:1032-1040.
31. Engel S, Isenmann S, Stander M, Rieger J, Bahr M, Weller M: Inhibition of experimental rat glioma growth by decorin gene transfer is associated with decreased microglial infiltration. *J Neuroimmunol* 1999, 99:13-18.
32. Roth JM, Akalu A, Zelmanovich A, Pollicarpo D, Ng B, MacDonald S, Formenti S, Liebes L, Brooks PC: Recombinant alpha2(IV)NC1 domain inhibits tumor cell-extracellular matrix interactions, induces cellular senescence, and inhibits tumor growth *in vivo*. *Am J Pathol* 2005, 166:901-911.
33. He GA, Luo JX, Zhang TY, Wang FY, Li RF: Canstatin-N fragment inhibits *in vitro* endothelial cell proliferation and suppresses *in vivo* tumor growth. *Biochem Biophys Res Commun* 2003, 312:801-805.
34. He GA, Luo JX, Zhang TY, Hu ZS, Wang FY: The C-terminal domain of canstatin suppresses *in vivo* tumor growth associated with proliferation of endothelial cells. *Biochem Biophys Res Commun* 2004, 318:354-360.
35. Panka DJ, Mier JW: Canstatin inhibits Akt activation and induces Fas-dependent apoptosis in endothelial cells. *J Biol Chem* 2003, 278:37632-37636.
36. Sudhakar A, Sugimoto H, Yang C, Lively J, Zeisberg M, Kalluri R: Human tumstatin and human endostatin exhibit distinct antiangiogenic activities mediated by alpha v beta 3 and alpha 5 beta 1 integrins. *Proc Natl Acad Sci USA* 2003, 100:4766-4771.
37. Boehm T, Folkman J, Browder T, O'Reilly MS: Antiangiogenic therapy of experimental cancer does not induce acquired drug resistance. *Nature* 1997, 390:404-407.
38. Sorensen DR, Read TA, Porwol T, Olsen BR, Timpl R, Sasaki T, Iversen PO, Benestad HB, Sim BK, Bjerkvig R: Endostatin reduces vascularization, blood flow, and growth in a rat gliosarcoma. *Neuro-oncol* 2002, 4:1-8.
39. Kim YM, Jang JW, Lee OH, Yeon J, Choi EY, Kim KW, Lee ST, Kwon YG: Endostatin inhibits endothelial and tumor cellular invasion by blocking the activation and catalytic activity of matrix metalloproteinase. *Cancer Res* 2000, 60:5410-5413.
40. Lee SJ, Jang JW, Kim YM, Lee HI, Jeon JY, Kwon YG, Lee ST: Endostatin binds to the catalytic domain of matrix metalloproteinase-2. *FEBS Lett* 2002, 519:147-152.
41. Nyberg P, Heikkila P, Sorsa T, Luostarinen J, Heljasvaara R, Stenman UH, Pihlajaniemi T, Salo T: Endostatin inhibits human tongue carcinoma cell invasion and intravasation and blocks the activation of matrix metalloproteinase-2, -9, and -13. *J Biol Chem* 2003, 278:22404-22411.
42. Dhanabal M, Ramchandran R, Waterman MJ, Lu H, Knebelmann B, Segal M, Sukhatme VP: Endostatin induces endothelial cell apoptosis. *J Biol Chem* 1999, 274:11721-11726.
43. Yokoyama Y, Dhanabal M, Griffioen AW, Sukhatme VP, Ramakrishnan S: Synergy between angioostatin and endostatin: Inhibition of ovarian cancer growth. *Cancer Res* 2000, 60:2190-2196.
44. Dkhissi F, Lu H, Soria C, Opolon P, Griscelli F, Liu H, Khattar P, Mshah Z, Perricaudet M, Li H: Endostatin exhibits a direct antitumor effect in addition to its antiangiogenic activity in colon cancer cells. *Hum Gene Ther* 2003, 14:997-1008.
45. Shinoura N, Hamada H: Gene therapy using an adenovirus vector for apoptosis-related genes is a highly effective therapeutic modality for killing glioma cells. *Curr Gene Ther* 2003, 3:147-153.
46. Puduvalli VK, Sawaya R: Antiangiogenesis-therapeutic strategies and clinical implications for brain tumors. *J Neurooncol* 2000, 50:189-200.
47. Jansen M, de Witt Hamer PC, Witmer AN, Troost D, van Noorden CJ: Current perspectives on antiangiogenesis strategies in the treatment of malignant gliomas. *Brain Res Brain Res Rev* 2004, 45:143-163.
48. De Boudard S, Guillamo JS, Christov C, Lefevre N, Brugieres P, Gola E, Devanz P, Indraco S, Peschanski M: Antiangiogenic therapy against experimental glioblastoma using genetically engineered cells producing interferon-alpha, angioostatin, or endostatin. *Hum Gene Ther* 2003, 14:883-895.
49. Ehteshami M, Black KL, Yu JS: Recent progress in immunotherapy for malignant glioma: treatment strategies and results from clinical trials. *Cancer Control* 2004, 11:192-207.
50. Peroullis I, Jonas N, Saleh M: Antiangiogenic activity of endostatin inhibits C6 glioma growth. *Int J Cancer* 2002, 97:839-845.
51. Pulkkanen KJ, Laukkanen JM, Fuxe J, Kettunen MI, Rehn M, Kannasto JM, Parkkinen JJ, Kauppinen RA, Pettersson RF, Yla-Herttuala S: The combination of HSV-tk and endostatin gene therapy eradicates orthotopic human renal cell carcinomas in nude mice. *Cancer Gene Ther* 2002, 9:908-916.
52. Visted T, Lund-Johansen M: Progress and challenges for cell encapsulation in brain tumour therapy. *Expert Opin Biol Ther* 2003, 3:551-561.
53. Ohlfest JR, Demorest ZL, Motooka Y, Vengco I, Oh S, Chen E, Scapaticci FA, Saplis RJ, Ekker SC, Low WC, Freese AB, Largaespada DA: Combinatorial antiangiogenic gene therapy by nonviral gene transfer using the sleeping beauty transposon causes tumor regression and improves survival in mice bearing intracranial human glioblastoma. *Mol Ther* 2005, 12:778-788.
54. Barnett FH, Scharer-Schulz M, Wood M, Yu X, Wagner TE, Friedlander M: Intra-arterial delivery of endostatin gene to brain tumors prolongs survival and alters tumor vessel ultrastructure. *Gene Ther* 2004, 11:1283-1289.
55. Rubenstein M, Shaw M, Mirochnick Y, Slobodskoy L, Glick R, Lichtor T, Chou P, Guinan P: *In vivo* establishment of T98G human glioblastoma. *Methods Find Exp Clin Pharmacol* 1999, 21:391-393.
56. Teicher BA, Menon K, Alvarez E, Galbreath E, Shih C, Faul M: Antiangiogenic and antitumor effects of a protein kinase Cbeta inhibitor in human T98G glioblastoma multiform xenografts. *Clin Cancer Res* 2001, 7:634-640.

Publish with **BioMed Central** and every scientist can read your work free of charge

"BioMed Central will be the most significant development for disseminating the results of biomedical research in our lifetime."

Sir Paul Nurse, Cancer Research UK

Your research papers will be:

- available free of charge to the entire biomedical community
- peer reviewed and published immediately upon acceptance
- cited in PubMed and archived on PubMed Central
- yours — you keep the copyright

Submit your manuscript here:
http://www.biomedcentral.com/info/publishing_adv.asp



アテロコラーゲン siRNA 導入技術の RNAi 医薬への応用

本間紀美,^{a,b} 竹下文隆,^a 落谷孝広^{*,a}

Application of Atelocollagen-mediated siRNA Delivery for RNAi Therapies

Kimi HONMA,^{a,b} Fumitaka TAKESHITA,^a and Takahiro OCHIYA^{*,a}

^aSection for Studies on Metastasis, National Cancer Center Research Institute, 5-1-1 Tsukiji, Chuo-ku, Tokyo 104-0045, Japan, and ^bKoken Bioscience Inst., KOKEN Co., Ltd., 2-13-10 Ukima, Kita-ku, Tokyo 115-0051, Japan

(Received January 5, 2007)

RNAi has rapidly become a powerful tool for drug target discovery and validation in an *in vitro* culture system and, consequently, interest is rapidly growing for extension of its application to *in vivo* systems, such as animal disease models and human therapeutics. Novel treatments and drug discovery in pre-clinical studies based on RNAi are currently targeting a wide range of diseases, including viral infections and cancers by the local administration of synthetic small interfering RNA (siRNA) that target local lesions. Recently, specific methods for the systemic administration of siRNAs have been reported to treat non-human primates or a cancer metastasis model. *In vivo* siRNA-delivery technology is a key hurdle to the successful therapeutic application of RNAi. This article reviews the non-viral delivery system of atelocollagen for siRNA, which could be useful for functional screening of the genes *in vitro* and *in vivo*, and will provide a foundation for further development of RNAi therapeutics.

Key words—RNAi; siRNA; atelocollagen; delivery

1. はじめに

RNA 干渉 (RNAi) は、植物でみつかった転写後遺伝子サイレンシング (post-transcriptional gene silencing; PTGS) あるいは、ウイルス誘発性遺伝子サイレンシング (viral-induced gene silencing; VIGS) という現象を手掛かりとして発見された。RNAi が線虫で初めて見出されたのは、1998 年のことであるが、相ついで、ゼブラフィッシュ、ショウジョウバエなど様々な種で確認され、さらに哺乳類においても RNAi が報告された。RNAi は、生物学や医学の研究に大きなインパクトを与えたと同時に、バイオ医療の新星として大いに注目されていることは、2006 年のノーベル医学生理学賞の受賞でも示されている。創薬においては、RNAi が遺伝子発現抑制による強力な解析ツールとして、新規治療標的の同定のために使用されている。また、医療においては、

siRNA (small interfering RNA) の患部への局所投与による、加齢黄斑変性症の治療が臨床試験段階にあるほか、感染症、がんを始めとした多くの疾患への適用が検討されている。近年、siRNA の全身投与によっても、霊長類における成功や、¹⁾ 転移性がんモデルでの成功が報告されており、²⁾ 臨床応用への期待が高まっている。

本総説では、われわれが開発したアテロコラーゲンによる siRNA 導入技術を中心に、アテロコラーゲンセルトランスフェクションアレイによる新規分子標的探索のためのユニークな解析手法、医療への応用も期待される生体への siRNA デリバリー方法について概説する。

2. RNAi

RNAi とは 2 本鎖 RNA (dsRNA) によって引き起こされる配列特異的な遺伝子発現抑制の現象である。生体内に導入された dsRNA は、RNase III ファミリーに属する Dicer と呼ばれる酵素により、3' 末端側に 2 塩基の突出を持つ 21 塩基の dsRNA である siRNA (short interfering RNA) にプロセッシングされる。siRNA は RNA-ヌクレアーゼ複合体

^a国立がんセンター研究所がん転移研究室 (〒104-0045 東京都中央区築地 5-1-1), ^b錫高研 高研バイオサイエンス研究所 (〒115-0051 北区浮間 2-13-10)

*e-mail: tochiya@ncc.go.jp

本総説は、日本薬学会第 126 年会シンポジウム S2 で発表したものを中心に記述したものである。

である RISC (RNA induced silencing complex) によって 2 本鎖がときほぐされたのちにアンチセンス鎖が取り込まれて、そのアンチセンス鎖に相補的な配列を持つ RNA を選択的に分解する。

RNAi は、以下の理由により、急速に普及し、核酸医薬としての実用化に期待が集まっている。siRNA は、1) 標的遺伝子に対する高い特異性を持つ、2) リスクに取り込まれた 1 本鎖 RNA は使い捨てではなく、連続して標的遺伝子を攻撃するため、毒性の生じ難いごく微量で確実な抑制効果を生む、3) 確実に標的遺伝子の発現を抑制し得る siRNA のデザインが、簡単なソフトによる検索で、誰にでも簡単に行える。この RNAi に先行して進んでいたのが同じ核酸医薬として開発されていたアンチセンス医薬である。しかし、副作用を上回るほどの有効性を示す臨床上的結果が得られず、最終的な承認に届かなかった例が多い。RNAi 医薬は、その抑制の確かさから、アンチセンス医薬に比べ、実用化において優位であると考えられている。一方で、その研究の歴史が浅いゆえに、メカニズムを完全に解明できたとは言えず、思わぬ副作用を招くことがないよう、臨床応用には慎重さが求められるのも事実である。

RNAi 医薬が実用化されるまでに残された課題の 1 つは、siRNA のデリバリー方法である。siRNA のデリバリーについては、動物個体レベルでも既に多くの試みがなされている。例えばマウスの尾静脈から合成 siRNA を体重の 10% もの大量の PBS 溶液で数秒の短時間で注入するハイドロダイナミック導入法で、動物の肝細胞への siRNA の導入に成功したとの報告がある。しかし、このような生体のホメオスタシスを無視した方法はヒトには到底適応できるものではない。また、ウイルスベクターに siRNA を組み込んで、動物個体に投与し siRNA を発現させる方法も開発されているが、まだ、臨床応用可能な方法は確立されていない。リポソーム製剤も siRNA 用に開発が進んでおり、霊長類における成功など、有望な成果も得られているが、アンチセンス医薬のデリバリーで問題になった、副作用については未知数である。われわれは、導入効率のみならず安全面でも優れる siRNA のデリバリーを指向し、アテロコラーゲンによる siRNA 導入技術の開発を進めている。以下に、アテロコラーゲンによる

siRNA デリバリーの有用性と課題について考察する。

3. アテロコラーゲン

アテロコラーゲン (Atelocollagen, 髙研) は、ウシ真皮の I 型コラーゲンを由来とするバイオマテリアルである。コラーゲン分子は、N-, C- 両末端にコラーゲンの主要抗原部位であるテロペプチドを有する。アテロコラーゲンは、そのテロペプチドを、ペプシン処理により除去した分子である。したがって、アテロコラーゲンは、免疫原性が極めて低く、生体適合性が高いバイオマテリアルである。それゆえ、長年医療分野で使用されてきたほか、DDS の基材としての応用研究も進められている。

4. アテロコラーゲンによる siRNA デリバリー

アテロコラーゲンによる核酸導入技術は、落谷らによって初めて発見された。³⁾以降、プラスミド DNA、アデノウィルスベクター、アンチセンスオリゴヌクレオチド、siRNA などが、アテロコラーゲンを導入担体とすることで、培養細胞及び生体に導入できることが報告されている。⁴⁻¹²⁾

生理的条件において、アテロコラーゲンは正電荷、siRNA などの核酸は負電荷を帯びるため、アテロコラーゲンと核酸の両者は、静電的に結合し複合体を形成する。アテロコラーゲンと核酸の複合体の形状は、主にアテロコラーゲンの濃度によって規定され、アテロコラーゲンの濃度の上昇とともに、粒子状から繊維状に変化する。⁴⁾アテロコラーゲンと核酸の複合体の形状は、デリバリーの効率に大きく影響し、デリバリー対象に応じて、適切な形状が存在する。われわれは、核酸デリバリーの際のアテロコラーゲン濃度を、培養細胞においては 80 $\mu\text{g}/\text{ml}$ 、生体における局所投与では 5000 $\mu\text{g}/\text{ml}$ 、全身投与では 500 $\mu\text{g}/\text{ml}$ に設定しており、良好な結果を得ている。

アテロコラーゲンと複合体化した核酸は、ヌクレアーゼによる分解を免れ、組織や細胞内に効率よく送達される。^{3,10)}アテロコラーゲンと核酸のコンプレックスはエンドソトーシスにより、細胞内に取り込まれると推定されている。siRNA は、RNase によって分解されてしまうため、いかに分解を防ぎ完全な分子状態を保つか、デリバリーの成否を決定付ける大きなポイントである。アテロコラーゲンと複合体を形成している siRNA は、血清及び生体組

織内で安定に保持されることが明らかとなっており,¹⁰⁾ アテロコラーゲン分子がヌクレアーゼの siRNA への接触をブロックしていると考えられている。

5. アテロコラーゲンセルトランスフェクションアレイ

ヒトゲノム解読後、遺伝子発現解析により、疾患や分化、発生など様々な生命現象に関する膨大な遺伝子発現情報をもたらされ、創薬においても、遺伝子の機能を細胞レベルで解析するファンクショナルゲノミクスの重要性が増しているのは言うまでもない。RNAiによる Loss of function の解析手法は、ファンクショナルゲノミクスのための強力なツールである。われわれは、RNAiによる遺伝子機能解析及び siRNA 医薬のスクリーニングに、アテロコラーゲンセルトランスフェクションアレイを使用している。^{4,11,13,14)} アテロコラーゲンセルトランスフェクションアレイとは、アテロコラーゲンによる核酸導入技術を、培養細胞へのハイスループットトランスフェクションに応用したシステムである。

従来、遺伝子導入は、あらかじめ細胞を培養しておき、そこに核酸と遺伝子導入試薬の混合物を慎重に調製し添加する、あるいはウイルスベクターを作製し感染させることで行われてきた。しかし、多検体の遺伝子を導入するのは、多大な時間と労力を要する。そこで開発されたのが、リバーストランスフェクションに基づくトランスフェクションアレイ技術である。リバーストランスフェクションは、あらかじめ導入可能な状態の核酸を基板上にアレイ化しておき、そこに細胞を播種して、細胞内に取り込ませる方法である。トランスフェクションアレイは、2001年にわれわれの研究グループと MIT の Sabatini ら 2つのグループが発表して以来、¹⁵⁾ 複数のグループが類似のシステムを考案している。

アテロコラーゲンセルトランスフェクションアレイは、アテロコラーゲンと siRNA のコンプレックスがマルチウェルプレートのウェルにコーティングされており、そこに細胞を播種、培養すると、細胞中に siRNA がトランスフェクションされる。あらかじめアテロコラーゲンと多検体の核酸とのコンプレックスを、96穴や 384穴などのマルチウェルプレートの各ウェルにアレイ化しておけば、多検体の siRNA を短時間で同時にトランスフェクションす

ることができる。さらに、培養終了後、既存の解析装置や各種測定試薬を使用して細胞機能解析を行うことで、ハイスループットな遺伝子機能解析が可能となる (Fig. 1)。

今までの遺伝子機能解析では、発現解析により同定された多検体の遺伝子をデータベース検索し、期待される機能を持つ少数の遺伝子に選抜した上で、その機能を解析するということが行われてきた。しかし、この方法では選抜されなかった他大多数の遺伝子について、機能を解明することはできない。また、期待される機能を持つ遺伝子に始めから絞り込んでしまっただけでは、他の遺伝子の持つ新規機能や新規

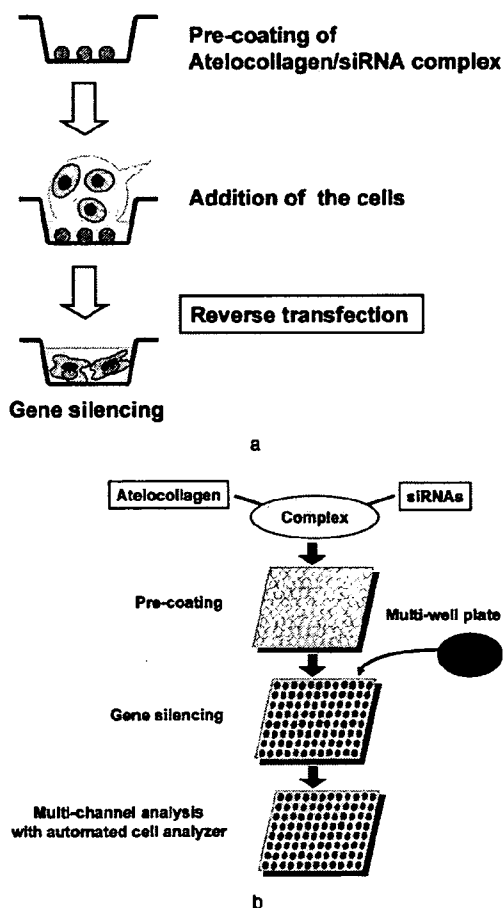


Fig. 1. Atelocollagen Based-cell Transfection Array

a: Principle of atelocollagen-based RNAi cell transfection array. Atelocollagen and siRNA complexes are pre-coated on a cell culture plate. The cells are added to the plate and then cells uptake the siRNAs by reverse transfection. Finally, RNAi-mediated gene silencing is induced in the cells. b: High-throughput Screening of Gene Function. The siRNA/atelocollagen complexes are arrayed and pre-coated on multi-well plates. The cells are plated into the siRNA/atelocollagen-complex pre-coated plates. After that, the effects of the downregulation of genes are evaluated with automated cell analyzer. Many genes function can be identified in a short time by atelocollagen-based cell transfection array.

遺伝子を突止めることはできない。やはり、発現解析により同定された多検体の遺伝子すべてについて、網羅的な遺伝子機能解析をすることが必要である。アテロコラーゲンセルトランスフェクションアレイは、網羅的な遺伝子機能解析を可能とする有力なシステムである。アテロコラーゲンセルトランスフェクションアレイで選ばれた有望な遺伝子については、次項より解説する。アテロコラーゲンによる生体への siRNA デリバリーで検証し、有力な分子標的となり得るものを同定することができる。アテロコラーゲン siRNA 導入技術を駆使した、*in vitro*, *in vivo* の解析は、新規分子標的を探索するための強力な戦略であるといえる (Fig. 2)。

6. 生体への siRNA デリバリー—局所投与—

アテロコラーゲンを導入担体とする siRNA の局所投与は、担がんマウスに対して、腫瘍に直接 siRNA とアテロコラーゲンの複合体を投与することで、複数の研究グループが良好な結果を得ている (Table 1)。われわれは、マウスの皮下に移植したメラノーマや精巣に移植した腫瘍に対し、アテロコラーゲンをを用いて siRNA を投与した結果、標的遺伝子の発現抑制を認め、RNAi 効果を確認した。¹⁰⁾ また、siRNA をアテロコラーゲンとともに複合体化することで、siRNA 単独で投与した場合よりも、RNAi 効果が持続し、より高い腫瘍増殖抑制効果を示すことを見出した。さらに、武井らは、ヌードマウスの皮下に移植したヒト前立腺がん細胞に対して、VEGF に対する siRNA とアテロコラーゲンの複合体を投与し、腫瘍の増殖を顕著に抑制できることを報告した。¹⁶⁾ その機序として、アテロコラーゲンの複合体の形成により、細胞への取り込み効率が高まるとともに、siRNA の半減期が延長されることが示されている。

7. 生体への siRNA デリバリー—全身投与—

アテロコラーゲンを導入担体とする siRNA の全身投与の有効性は、腫瘍の骨転移モデルで確かめられている。²⁾ われわれは、ヒト前立腺がん細胞を、ヌードマウスの左心室に移植して骨転移モデルを製作し、尾静脈投与によって siRNA とアテロコラーゲン複合体が、骨を含めた全身の転移巣へとデリバリーされるかを検討した。siRNA 単独投与では標的遺伝子産物の抑制効果は 40% 以下であるのに対し、siRNA とアテロコラーゲンの複合体の投与では、90% 以上の抑制効果を認めた。この結果は、骨

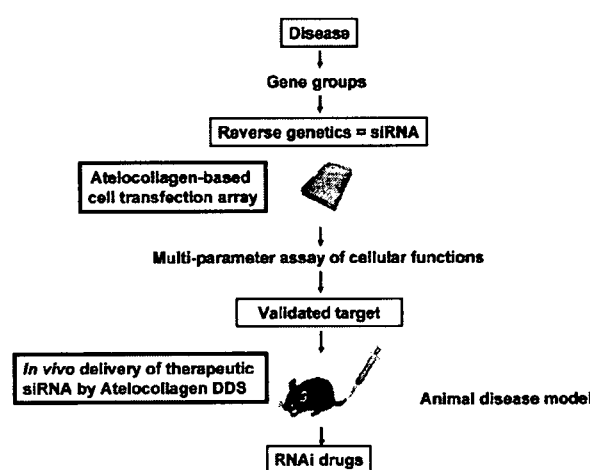


Fig. 2. The Strategy for the Target Validation of Druggable Genes by an Atelocollagen-based siRNA Delivery *In vitro* and *In vivo*

The Based on information about gene groups (several hundred in a pool) that possess altered expression levels (increased) in diseases as detected by microarray analyses of clinical samples, we synthesize siRNAs against genes. These siRNA molecules are screened using an atelocollagen-based cell transfection array on target culture cells (a cell line), and then identified the siRNAs that induce the desired activities, such as apoptosis, cell proliferation, or infiltration. Next, we use atelocollagen DDS to deliver these candidate siRNAs into animals that serve as models of diseases. Finally, drug actions are examined to identify the druggable molecules that can be clinically applied to humans.

Table 1. *In vivo* Delivery of siRNAs by Atelocollagen

Therapeutic model (Cell lines)	Implanted site (Target organs)	Route	Target genes	References
Prostate cancer (PC-3)	s.c.	<i>i.t.</i>	VEGF	16
Germ-cell tumor (NEC8)	Testis	<i>i.t.</i>	FGF-4	10
Prostate cancer (PC-3M-Luc)	Bone metastasis	<i>i.v.</i>	EZH2, p110a	2
Prostate cancer (PC-3)	s.c.	<i>i.t.</i>	midkine	17
Cervical cancer	s.c.	<i>i.t.</i>	HPV18 (E6 & E7)	18
Head and neck squamous cell carcinoma (SAS)	s.c.	<i>i.t.</i>	EGFR	19

s.c.: subcutaneous, *i.v.*: intravenous, *i.t.*: intratumoral.

転移巣をターゲットとした全身性のデリバリーにも、アテロコラーゲンが適用可能であることを示している。また、前立腺がんの悪性度に関与する2つの遺伝子、EZH2とp110 α に対するsiRNAのアテロコラーゲンによるデリバリーは、骨転移腫瘍の増殖を顕著に抑制することも確認した。さらに、アテロコラーゲンによるsiRNAのデリバリーは、インターフェロンやインターロイキンなどの有害な反応を惹起せず、その安全性が示された。

8. アテロコラーゲン siRNA デリバリーシステムの課題

生体への核酸デリバリーにおけるキーポイントの1つはいかに正常部位への影響を少なくして、標的とする病巣部にのみ核酸を送達するかである。アテロコラーゲン DDS による siRNA の全身投与では、先の骨転移モデルマウスにおいて、骨転移腫瘍部位と同時に、正常の他の臓器へも siRNA がデリバリーされることが確認された。²⁾ また、正常の動物に全身性に投与すると、複合体である siRNA の動態は、多くの臓器に分布する結果となり、標的性や目立った臓器指向性はなさそうである。アテロコラーゲン DDS による全身性投与方法もヒトへの応用に関してはまだ越えるべき大きな壁があるといえる。

一方で、担がんマウスへのアテロコラーゲン siRNA の全身性投与では、同じ動物の腫瘍部位への siRNA の到達度は、正常な肝臓と比較して、およそ 1.7—2.2 倍であった。この腫瘍への siRNA の到達度の違いは 1986 年に前田らによって見いだされた EPR 効果 (Enhanced Permeation and Retention effect) によって一部説明することが可能かもしれない。²⁰⁾ EPR 効果とは、がん組織にある新生血管は正常組織の血管に比べて、血管壁組織の構築性が悪く、物質透過性が高いため、サイズの比較的大きな高分子化合物がより多くがん組織に透過・移行する。さらに、がん組織ではリンパ管による高分子化合物の回収機構が不完全であると考えられるため、高分子化合物はがん組織内に滞留し易くなる効果のことである。実際、アテロコラーゲンを用いた siRNA デリバリーによる遺伝子発現の抑制効果は、正常組織よりもがん組織で大きいことが確認されている。この EPR 効果の発見により、固形がんに対するターゲティング研究は大きく変化した。従来、がん細胞への薬物のターゲティングの研究

開発は、これまでがん細胞に特異的に発現している抗原との抗体反応を利用し薬剤をがんのみに集積させようとするアクティブターゲティングの原理に基づいて行われてきた。しかし、標的とするがん抗原に類似の抗原が血液中及び他の正常細胞表面に存在するため、標的部位に薬物を薬効の出る一定濃度以上に集積できないという問題があった。EPR 効果を利用した、がん細胞に血中の薬物を取り込ませるパッシブターゲティングは、この問題を克服する手掛かりとなるかもしれない。アテロコラーゲン DDS と EPR 効果の関係を検討することには、がん治療への応用に向けて、大きな意味を持つと考えられる。

9. おわりに

本稿では、アテロコラーゲンによる siRNA 導入技術が、アテロコラーゲンセルトランスフェクションアレイによる新規分子標的探索に応用されること、生体への siRNA デリバリーに有用であることを述べた。しかし、アテロコラーゲンと siRNA 複合体の細胞内への取り込み過程や RNAi 効果の長期維持に関する分子レベルでの解明、生体における標的性の向上など、重要な課題も残されている。また、siRNA と並んで RNAi 創薬として、注目されているのが microRNA (miRNA) である。miRNA は翻訳レベルでタンパク質の発現を制御しているとされ、ヒトでは 500 種類以上の miRNA が同定されている。miRNA の発現異常が、がんなどの疾患に関与することが明らかとなってきた。この miRNA に関しても、それらが制御する疾患の解明や治療への糸口として、アテロコラーゲンによるデリバリーの応用が有効かも知れない。われわれは、これらの課題を解決し、アテロコラーゲンによる核酸デリバリーが、導入効率と安全性の高い DDS として、医療分野で実用化されることを目指している。

謝辞 本研究成果は、国立がんセンター研究所がん転移研究室、(株)高研、大日本住友製薬の共同研究による。

REFERENCES

- 1) Zimmermann T. S., Lee A. C., Akinc A., Bramlage B., Bumcrot D., Fedoruk M. N., Harborth J., Heyes J. A., Jeffs L. B., John

- M., Judge A. D., Lam K., McClintock K., Nechev L. V., Palmer L. R., Racie T., Rohl I., Seiffert S., Shanmugam S., Sood V., Soutschek J., Toudjarska I., Wheat A. J., Yaworski E., Zedalis W., Koteliensky V., Manoharan M., Vornlocher H. P., MacLachlan I., *Nature*, **441**, 11–14 (2006).
- 2) Takeshita F., Minakuchi Y., Nagahara S., Honma K., Sasaki H., Hirai K., Teratani T., Namatame N., Yamamoto Y., Hanai K., Kato T., Sano A., Ochiya T., *Proc. Natl. Acad. Sci. U.S.A.*, **102**, 12177–12182 (2005).
 - 3) Ochiya T., Takahama Y., Nagahara S., Sumita Y., Hisada A., Itoh H., Nagai Y., Terada M., *Nat. Med.*, **5**, 707–710 (1999).
 - 4) Honma K., Ochiya T., Nagahara S., Sano A., Yamamoto H., Hirai K., Aso Y., Terada M., *Biochem. Biophys. Res. Commun.*, **289**, 1075–1081 (2001).
 - 5) Ochiya T., Nagahara S., Sano A., Itoh H., Terada M., *Curr. Gene Ther.*, **1**, 31–52 (2001).
 - 6) Hirai K., Sasaki H., Sakamoto H., Takeshita F., Asano K., Kubota Y., Ochiya T., Terada M., *J. Gene Med.*, **5**, 951–957 (2003).
 - 7) Sano A., Maeda M., Nagahara S., Ochiya T., Honma K., Itoh H., Miyata T., Fujioka K., *Adv. Drug Deliv. Rev.*, **55**, 1651–1677 (2003).
 - 8) Nakamura M., Ando Y., Nagahara S., Sano A., Ochiya T., Maeda S., Kawaji T., Ogawa M., Hirata A., Terazaki H., Haraoka K., Tanihara H., Ueda M., Uchino M., Yamamura K., *Gene Ther.*, **11**, 838–846 (2004).
 - 9) Hanai K., Kurokawa T., Minakuchi Y., Maeda M., Nagahara S., Miyata T., Ochiya T., Sano A., *Hum. Gene Ther.*, **15**, 263–272 (2004).
 - 10) Minakuchi Y., Takeshita F., Kosaka N., Sasaki H., Yamamoto Y., Kouno M., Honma K., Nagahara S., Hanai K., Sano A., Kato T., Terada M., Ochiya T., *Nucleic Acids Res.*, **32**, e109 (2004).
 - 11) Honma K., Miyata T., Ochiya T., *Curr. Drug Discov. Technol.*, **1**, 287–294 (2004).
 - 12) Takeshita F., Ochiya T., *Cancer Sci.*, **97**, 689–696 (2006).
 - 13) Saito S., Honma K., Kita-Matsuo H., Ochiya T., Kato K., *Physiol. Genomics*, **22**, 8–13 (2005).
 - 14) Kurokawa Y., Honma K., Takemasa I., Nakamori S., Kita-Matsuo H., Motoori M., Nagano H., Dono K., Ochiya T., Monden M., Kato K., *Int. J. Oncol.*, **28**, 383–391 (2006).
 - 15) Ziauddin J., Sabatini D. M., *Nature*, **411**, 107–110 (2001).
 - 16) Takei Y., Kadomatsu K., Yuzawa Y., Matsuo S., Muramatsu T., *Cancer Res.*, **64**, 3365–3370 (2004).
 - 17) Takei Y., Kadomatsu K., Goto T., Muramatsu T., *Cancer*, **107**, 864–873 (2006).
 - 18) Fujii T., Saito M., Iwasaki E., Ochiya T., Takei Y., Hayashi S., Ono A., Hirao N., Nakamura M., Kubushiro K., Tsukazaki K., Aoki D., *Int. J. Oncol.*, **29**, 541–548 (2006).
 - 19) Nozawa H., Tadakuma T., Ono T., Sato M., Hiroi S., Masumoto K., Sato Y., *Cancer Sci.*, **97**, 1115–1124 (2006).
 - 20) Maeda H., Wu J., Sawa T., Matsumura Y., Hori K., *J. Control. Release*, **65**, 271–284 (2000).

Effects of Dietary Cholesterol on Tissue Ceramides and Oxidation Products of Apolipoprotein B-100 in ApoE-Deficient Mice

Ikuyo Ichi · Yuka Takashima · Noriko Adachi ·
Kayoko Nakahara · Chiaki Kamikawa ·
Mariko Harada-Shiba · Shosuke Kojo

Received: 1 March 2007 / Accepted: 20 April 2007 / Published online: 24 July 2007
© AOCS 2007

Abstract Oxidized LDL (oxLDL) has been shown to activate the sphingomyelinase pathway producing ceramide in vascular smooth muscle cells. Therefore ceramide, which is a biologically active lipid causing apoptosis in a variety of cells, may be involved in the apoptotic action of oxLDL. In this study, we examined whether cholesterol enriched diets affected ceramide metabolism and oxidation product of LDL, represented by degradation of apolipoprotein B-100 (apoB) in apoE-deficient (apoE^{-/-}) mice. ApoE^{-/-} and wild type mice were fed a standard (AIN-76) diet or 1% cholesterol-enriched diet for 8 weeks. Tissue ceramide levels were analyzed using electrospray tandem mass spectrometry (LC-MS/MS). Ceramide levels in the plasma and the liver of apoE^{-/-} mice were intrinsically higher than those of the wild type. In apoE^{-/-} mice, dietary cholesterol significantly increased several ceramides and degradation products of apoB in plasma compared to those fed the control diet. Dietary cholesterol did not affect tissue ceramide levels in the wild type mice. Based on these results, plasma ceramides possibly correlate with the increase in LDL oxidation and are a risk factor for atherosclerosis.

Keywords Ceramide · Cholesterol ·
Apolipoprotein B-100 · Oxidation · LC-MS/MS

I. Ichi · Y. Takashima · N. Adachi · K. Nakahara ·
C. Kamikawa · S. Kojo (✉)
Department of Food Science and Nutrition,
Nara Women's University, Nara 630-8506, Japan
e-mail: kojo@cc.nara-wu.ac.jp

M. Harada-Shiba
Department of Bioscience,
National Cardiovascular Center Research Institute,
Osaka 565-8565, Japan

Abbreviations

ApoB	apolipoprotein B-100
ApoE ^{-/-}	apoE deficient
IMT	Intima-media thickness of the carotid artery
LDL	Low-density lipoprotein
oxLDL	oxidized LDL
SDS-PAGE	Sodium dodecyl sulfate polyacrylamide gel electrophoresis
SM	Sphingomyelin
SMase	Sphingomyelinase
SPT	Serine palmitoyl-CoA transferase
TG	Triglyceride

Introduction

Ceramide has been implicated in regulating cell-cycle arrest, apoptosis, and cell senescence [1–3] and is reported to serve as an intracellular second messenger [4]. Therefore, ceramide has attracted much attention as a new lipid mediator. Ceramide consists of a fatty acid of C16–C26 chain length bound to the amino group of sphingosine. Ceramide is generated by sphingomyelin (SM) hydrolysis by sphingomyelinase (SMase) or by de novo synthesis starting from serine-palmitoyl transferase (SPT) [5]. A significant positive correlation was observed between plasma levels of SM and the severity of coronary heart disease [6], and plasma SM levels increased in human familial hyperlipidemias [7]. Recent studies have demonstrated correlations between sphingomyelin and atherogenic risk factors of plasma in humans [8] and inhibitions of de novo SM and ceramide biosynthesis reduced atherosclerotic lesion in apoE-deficient (apoE^{-/-}) mice [9, 10].

We recently showed that ceramide concentrations in human plasma had a significantly positive correlation with lipid markers that associated with atherosclerosis [11]. Plasma ceramide concentration increased drastically at a high level of LDL cholesterol (more than 170 mg/dL). Therefore, an increase in ceramide may be a risk factor for atherosclerosis, like LDL cholesterol.

Oxidative modification of LDL is an important factor in the development of atherosclerosis [12]. Although LDL is composed of lipids, protein, and sugar chains, studies on the oxidation of LDL have mainly focused on lipid peroxidation [13]. The protein part of LDL, apolipoprotein B-100 (apoB), is also reactive to radical oxidation and it undergoes fragmentation and conjugation [14, 15]. Among the plasma proteins, apoB is unusually reactive to radical reactions compared to albumin and transferrin and even comparable to vitamin E, a typical radical scavenger [14]. Thus, both fragmented and conjugated apoB proteins are present in normal human serum and these oxidation reaction products of LDL tend to increase with age [15]. In addition, we reported that B-ox, namely the sum of fragmented and conjugated apoB proteins determined by an immunoblot assay, showed a significant positive correlation with IMT (intima-media thickness of the carotid artery) and LDL cholesterol, and a negative correlation with HDL cholesterol, and vitamin C [15]. These reports suggest that B-ox is a reliable mechanism-based indicator of atherosclerosis.

Proteolytic degradation of apoB has been shown to cause aggregation and fusion of LDL [16]. Aggregated LDL in atherosclerotic lesions is proposed as representing a central process in atherosclerosis [17] and is enriched with ceramide [18]. Furthermore, LDL treated with SMase induces foam cell formation *in vitro* [18, 19]. Based on these reports, a correlation between ceramide and oxLDL is suggested.

Dietary cholesterol raises LDL cholesterol levels and a very high intake of cholesterol causes atherosclerosis. The activity of SPT, which catalyzes the first step in ceramide synthesis, is augmented in the aorta of rabbits fed high cholesterol diets [20]. Treatment of mice with myriocin, a specific inhibitor of SPT, lowered plasma cholesterol levels of ceramide in a dose-dependent manner. Therefore, high cholesterol diets may affect ceramide synthesis. The apoE^{-/-} mice exhibit high levels of plasma cholesterol as a result of impaired clearance of cholesterol-enriched lipoproteins [21]. Therefore, apoE^{-/-} mice are more sensitive to dietary cholesterol. In the present study, we examine the effect of high cholesterol diets on the ceramide levels in plasma, liver, and adipose tissues of apoE^{-/-} mice in comparison with wild-type mice. We also demonstrate that dietary cholesterol results in enhancement of oxidation of apoB, namely degradation of apoB, in apoE^{-/-} mice.

Experimental Procedures

Materials

All solvents were purchased from Wako Pure Chemicals Co. (Osaka, Japan). All other reagents were obtained from Funakoshi Co. (Tokyo, Japan). A commercially available diagnostic kit for cholesterol and triglyceride (TG) were purchased from Wako Pure Chem. Co. (Osaka, Japan). Silica gel 60 TLC plates were purchased from Merck (Darmstadt, Germany). A Vectastain ABC-PO (goat IgG) kit was purchased from Vector Lab. Inc. (Burlingame, CA, USA). Anti-human lipoprotein B goat IgG was purchased from Sigma Chem. Co. (St. Louis, MO, USA). Polyvinylidene difluoride (PVDF) membrane filters were purchased from Millipore (Tokyo, Japan). Electrophoresis reagents were purchased from Nacalai Tesque Inc. (Kyoto, Japan).

Animals and Diets

This study was approved by the Animal Care Committee of Nara Women's University. Eight-week-old male apoE^{-/-} mice on C57BL/6J background mice were purchased from Jackson Laboratories (Bar Harbor, Me., USA). Eight-week-old male C57BL/6J mice were also obtained from Japan SLC Co. (Hamamatsu, Shizuoka, Japan). The animals were housed in a room at 24 ± 2 °C, with a 12/12 h light–dark cycle. A standard diet was formulated according to the AIN-76 formula. The control group was fed a standard diet, and the cholesterol group was fed a standard diet supplemented with 1% cholesterol. Mice were randomized into the two groups. Mice were fed these experimental diets *ad libitum* for 8 weeks. All mice were starved for 6 h before killing.

Analytical Method

Mice were anesthetized with Nembutal, and blood samples were collected by right-ventricle puncture using a syringe containing sodium heparin as an anticoagulant. After perfusion, the liver and adipose tissues were dissected out. Blood was centrifuged to separate the plasma.

Plasma cholesterol and TG were measured using a commercially available diagnostic kit. Liver cholesterol concentration was analyzed by gas–liquid chromatography (GC-2014, Shimadzu, Kyoto, Japan) using 5 α -cholestane as an internal standard [22]. Liver TG was analyzed as described by Fletcher et al. [23]. Vitamin C was measured according to a specific and sensitive method involving chemical derivatization and HPLC [24].

Ceramide Analysis

Lipid of each tissue was extracted according to the method of Folch et al. [25]. Lipid in the liver and the adipose tissues was dissolved in chloroform to perform silica gel 60 TLC (Merck, Darmstadt, Germany). TLC separation was performed as previously described [26].

Quantitative measurement of ceramide species was made using a triple-quadrupole mass spectrometer (Finnigan MAT TSQ 7000). ESI-MS/MS was performed as previously described [11, 26]. HPLC was conducted with a μ -Bondasphere column (5 μ C18 100A Waters). Elution was performed at a flow rate of 0.2 ml/min with a mixture of 5 mM ammonium formate, methanol, and tetrahydrofuran at a volume ratio of 1:2:7. The mobile phase stream was connected to the ionspray interface of an ESI-MS/MS system. Standards and cellular ceramide extracts were stored at -20°C . Mass analysis was performed in the positive mode in a heated capillary tube at 250°C with an electrospray potential of 4.5 kV, a sheath gas pressure of 70 psi, and a collision gas pressure of 1.6–2.0 mtorr. Under optimized conditions, monitoring ions were ceramide molecular species $(\text{M}+\text{H})^{+}$ for the product ion at m/z 264 of the sphingoid base. Standards and samples were injected with 5 μl of 5 pmol C8:0-ceramide as an internal standard for ESI-MS/MS. The quantity of each ceramide was calibrated from each ceramide/C8:0-ceramide ratio, assuming that the calibration curve of ceramides bearing C16–24 acyl chains was similar to that of C16:0-ceramide as previously described [11, 26]. Each sample was analyzed in duplicate.

Western Blot Analysis

For electrophoresis, the sample was applied to 4% sodium dodecyl sulfate polyacrylamide gel electrophoresis (SDS-PAGE), and immunoblot analysis was performed, both as described previously [14, 15]. Proteins separated on the gel were electrophoretically transferred to PVDF membrane

filters and immunoblotting analyses of apoB were performed as previously described [14, 15].

Anti-mouse apoB antiserum was prepared by immunizing mouse LDL to a rabbit. Chemiluminescence was analyzed with ATTO Densitograph Software Library (CS Analyzer Ver2.0).

Statistical Analysis

The data were expressed as mean \pm SE. Differences between group means were considered significant at $P < 0.05$ using Fisher's protected least significant difference test (PLSD).

Results

Effect of Dietary Cholesterol on Body Weight and Lipids

The body weight of the apoE^{-/-} control group was higher than those of the other groups (Table 1). Liver weight of apoE^{-/-} mice was higher than that of the wild type control group. The weight of total white adipose tissue of the apoE^{-/-} control group was higher than those of the wild control group and the apoE^{-/-} cholesterol group. No differences were observed in daily food consumption among these four groups (data not shown).

Plasma cholesterol of apoE^{-/-} mice fed a control diet was about 6.7 times higher than that of the wild type mice fed a control diet (Table 2). In the cholesterol group, plasma cholesterol of the apoE^{-/-} mice was also about six times higher than that of the wild type mice. However, the liver cholesterol in the apoE^{-/-} mice was not different from that of the wild type mice. Cholesterol levels of plasma and the liver in both the wild type and the apoE^{-/-} mice fed cholesterol were higher than those in mice fed a diet without cholesterol. No difference was observed among all groups in plasma TG. However, the liver TG of the wild type control group was lower than that of the other groups.

Table 1 Effect of dietary cholesterol on weights of body, liver, and white adipose tissue (WAT) of wild type and apoE^{-/-} mice

	Wild control	Wild cholesterol	ApoE ^{-/-} control	ApoE ^{-/-} cholesterol
Body weight (g)	32.3 \pm 0.9 ^a	33.8 \pm 1.3 ^a	38.1 \pm 1.3 ^b	35.1 \pm 1.0 ^a
Liver weight (g)	1.30 \pm 0.09 ^a	1.67 \pm 0.12 ^{ac}	1.84 \pm 0.11 ^{bc}	1.84 \pm 0.18 ^{bc}
Epididymal WAT weight (g)	0.68 \pm 0.11 ^a	1.12 \pm 0.15 ^b	1.33 \pm 0.13 ^b	0.76 \pm 0.11 ^a
Perirenal WAT weight (g)	0.39 \pm 0.07 ^a	0.47 \pm 0.07 ^{ac}	0.68 \pm 0.08 ^b	0.38 \pm 0.08 ^a
Mesenteric WAT weight (g)	0.38 \pm 0.06 ^a	0.50 \pm 0.08 ^{ac}	0.63 \pm 0.06 ^{bc}	0.33 \pm 0.05 ^a
Total WAT weight (g)	1.49 \pm 0.21 ^a	2.08 \pm 0.30 ^{ac}	2.64 \pm 0.27 ^{bc}	1.44 \pm 0.22 ^a

The values were mean \pm SE for eight C57BL/6J and ten apoE^{-/-} mice. Differences between group means were considered significant at $P < 0.05$ using Fisher's protected least significant difference test (PLSD). Values with different superscript letters show significant difference at $P < 0.05$

Table 2 Effect of dietary cholesterol on plasma and liver lipids of wild type and apoE^{-/-} mice

	Wild control	Wild cholesterol	ApoE ^{-/-} control	ApoE ^{-/-} cholesterol
Plasma cholesterol (mg/dL)	77.4 ± 12.7 ^a	140 ± 11 ^a	517 ± 46 ^b	873 ± 64 ^c
Plasma triacylglycerol (mg/dL)	30.4 ± 1.9	28.6 ± 2.0	42.4 ± 6.3	46.6 ± 13.4
Liver cholesterol (mg/g)	3.36 ± 0.44 ^a	14.3 ± 1.9 ^b	5.76 ± 0.48 ^a	15.2 ± 1.4 ^b
Liver triacylglycerol (mg/g)	44.2 ± 8.8 ^a	115 ± 30 ^b	179 ± 25 ^b	119 ± 21 ^b

The values were mean ± SE for eight C57BL/6J and ten apoE^{-/-} mice. Differences between group means were considered significant at $P < 0.05$ using Fisher's protected least significant difference test (PLSD). Values with different superscript letters show significant difference at $P < 0.05$

Effect of Dietary Cholesterol on Ceramide

Table 3 shows the distribution of ceramide species in plasma. A major ceramide in plasma was C24:0 in both wild type and apoE^{-/-} mice. The plasma level of total ceramide of the apoE^{-/-} mice fed a control diet was about six times higher than that of the wild type mice fed a control diet. In the cholesterol group, the plasma level of total ceramide in the apoE^{-/-} mice was also about 5.1 times higher than that of the wild type mice. In apoE^{-/-} mice, the plasma level of total ceramide of the cholesterol group tended to be higher than that of the control group ($p = 0.08$), while C16:0, C24:1, and C24:2 of the cholesterol group were significantly higher than those of the control group. In the wild type mice, dietary cholesterol did not affect plasma levels of ceramide.

Table 4 shows the distribution of ceramide species in the liver. The major ceramide of the liver was also C24:0 in the wild type and the apoE^{-/-} mice. In the liver, the total ceramide of the apoE^{-/-} mice fed a control diet was about 1.5 times higher than that of the wild type mice fed a control diet. In the cholesterol group, the total ceramide of apoE^{-/-} mice was not different from that of the wild type mice. Thus, the difference in total ceramide level between

wild type and apoE^{-/-} mice in the liver was less than that in plasma. In addition, dietary cholesterol did not affect ceramide levels of the liver in either the wild type or the apoE^{-/-} mice.

Table 5 shows the distribution of ceramide species in the mesenteric white adipose tissue. Major ceramides of white adipose tissue were C24:0, C16:0, and C24:1. The ratio of C16:0 and C18:0 in adipose tissues was higher than that in plasma and the liver. In the wild type mice and the apoE^{-/-} mice fed cholesterol, the content of C16:0 of the adipose tissue was similar to that of C24:0. In the adipose tissue, the total ceramide of the wild type was not different from that of the apoE^{-/-} mice. In addition, dietary cholesterol did not affect ceramides of the adipose tissue in either wild type or apoE^{-/-} mice.

Effect of Dietary Cholesterol on Cross-Linked and Fragmented apoB

The band, which was larger than the band of apoB (512 kDa) was assumed to be a cross-linking product as previously reported [15] and the band, which was smaller than the band of apoB was assumed to be a fragmented product. However, neither cross-linking nor fragmentation

Table 3 Effect of dietary cholesterol on ceramide concentration (nmol/ml) in the plasma

	Wild control	Wild cholesterol	ApoE ^{-/-} control	ApoE ^{-/-} cholesterol
C16:0	0.75 ± 0.13 ^a	1.20 ± 0.18 ^a	4.11 ± 0.32 ^b	5.71 ± 0.42 ^c
C18:0	0.07 ± 0.01 ^a	0.10 ± 0.02 ^a	0.75 ± 0.11 ^b	0.85 ± 0.1 ^b
C22:0	3.05 ± 0.83 ^a	4.12 ± 0.80 ^a	25.5 ± 3.8 ^b	24.5 ± 3.3 ^b
C24:0	6.16 ± 1.54 ^a	9.04 ± 1.46 ^a	34.3 ± 2.8 ^b	41.5 ± 4.6 ^b
C24:1	3.36 ± 0.77 ^a	4.70 ± 0.98 ^a	15.3 ± 1.4 ^b	20.2 ± 2.2 ^c
C24:2	0.14 ± 0.03 ^a	0.22 ± 0.04 ^a	2.03 ± 0.38 ^b	5.01 ± 0.67 ^c
Total	13.4 ± 3.3 ^a	19.1 ± 3.3 ^a	80.6 ± 6.8 ^b	97.8 ± 11.0 ^b

The values were mean ± SE for eight C57BL/6J and ten apoE^{-/-} mice. Differences between group means were considered significant at $P < 0.05$ using Fisher's protected least significant difference test (PLSD). Values with different superscript letters show significant difference at $P < 0.05$

Table 4 Effect of dietary cholesterol on ceramide concentration (nmol/g tissue) in the liver

	Wild control	Wild cholesterol	ApoE ^{-/-} control	ApoE ^{-/-} cholesterol
C16:0	19.6 ± 3.0 ^a	22.3 ± 2.6 ^{ab}	28.5 ± 2.4 ^b	27.5 ± 3.2 ^b
C18:0	2.52 ± 0.5 ^a	2.16 ± 0.29 ^{ab}	3.90 ± 0.33 ^{ac}	4.36 ± 0.93 ^c
C22:0	38.4 ± 4.1 ^a	47.1 ± 5.1 ^a	80.6 ± 6.3 ^b	50.0 ± 4.9 ^{ac}
C24:0	75.0 ± 10.1 ^a	88.9 ± 6.5 ^{ab}	99.6 ± 7.4 ^b	97.7 ± 8.7 ^b
C24:1	50.3 ± 8.2	61.8 ± 5.5	63.1 ± 5.9	71.6 ± 6.3
C24:2	4.62 ± 0.84 ^a	5.57 ± 0.58 ^a	5.80 ± 0.74 ^a	9.59 ± 1.12 ^b
Total	190 ± 19 ^a	228 ± 17 ^{ab}	281 ± 19 ^b	261 ± 23 ^b

The values were mean ± SE for eight C57BL/6J and ten apoE^{-/-} mice. Differences between group means were considered significant at $P < 0.05$ using Fisher's protected least significant difference test (PLSD). Values with different superscript letters show significant difference at $P < 0.05$

Table 5 Effect of dietary cholesterol on ceramide concentration (nmol/g tissue) in the mesenteric white adipose tissues

	Wild control	Wild cholesterol	ApoE ^{-/-} control	ApoE ^{-/-} cholesterol
C16:0	51.4 ± 4.7	52.7 ± 15.0	43.8 ± 10.0	55.9 ± 9.3
C18:0	16.9 ± 3.5	19.7 ± 5.2	10.8 ± 1.8	19.9 ± 4.4
C22:0	21.1 ± 2.9	17.3 ± 3.2	15.4 ± 2.8	16.9 ± 2.9
C24:0	63.0 ± 10.4	53.3 ± 11.1	49.6 ± 11.1	56.5 ± 11.7
C24:1	53.8 ± 9.0	47.6 ± 9.2	40.1 ± 8.4	49.6 ± 9.8
C24:2	8.40 ± 1.41	7.68 ± 1.69	6.09 ± 1.05	10.2 ± 2.2
Total	215 ± 30	198 ± 45	159 ± 34	209 ± 38

The values were mean ± SE for eight C57BL/6J and ten apoE^{-/-} mice. Differences between group means were considered significant at $P < 0.05$ using Fisher's protected least significant difference test (PLSD). Values with different superscript letters show significant difference at $P < 0.05$

of apoB-48 (250 kDa) were detected (Fig. 1a). Western blot analysis of plasma revealed that apoB-100 with molecular weight of 512 kDa in the apoE^{-/-} cholesterol group was lower than that in the apoE^{-/-} control group (Fig. 1a, b). Though cross-linking of apoB-100 was not detected in apoE^{-/-} mice, fragmentation of apoB-100 in the apoE^{-/-} cholesterol group was 2.5 times higher than that in the apoE^{-/-} control group (Fig. 1c). In the wild type mice, neither cross-linked nor fragmented apoB proteins were discernible (data not shown).

The amount of the aortic area covered with plaques was significantly greater in the apoE^{-/-} mice fed cholesterol compared to the apoE^{-/-} mice fed a control diet, as is well established (data not shown).

Effect of Dietary Cholesterol on Vitamin C

In plasma, vitamin C of apoE^{-/-} mice was higher than that of wild type mice (Table 6). Vitamin C of both wild type and the apoE^{-/-} mice fed a cholesterol diet was higher than for mice fed a control diet.

Discussion

Sphingolipids such as ceramide and sphingosine-1-phosphate are bioactive lipid mediators [27]. The importance of sphingolipids as mediators in cardiovascular pathophysiology has recently been reported [28]. In addition, it was shown that SPT activity was higher in apoE^{-/-} mice compared with C57BL/6J mice [9]. In this study, it was shown that the total ceramide level in plasma and the liver of the apoE^{-/-} control group was higher than that of the wild control group. Therefore, decreasing ceramide levels in plasma and the liver may be beneficial for prevention of atherogenesis.

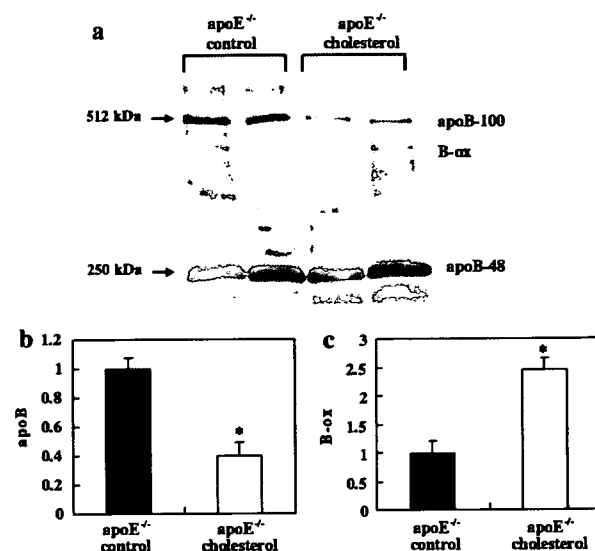


Fig. 1 ApoB and fragmented apoB-100 proteins in plasma of apoE^{-/-} mice fed a standard diet and supplemented with 1% cholesterol. Plasma was loaded on 4% SDS-PAGE gel and Western blot analysis was performed (a). Densitometry of apoB (b) and fragmented apoB (c) in plasma of apoE^{-/-} mice. The values were means ± SE for 4–5 apoE^{-/-} mice and asterisks indicated significant differences from the corresponding apoE^{-/-} control group

Table 6 Effect of dietary cholesterol on plasma Vitamin C concentration (nmol/mL) of wild type and apoE^{-/-} mice

	Wild control	Wild cholesterol	ApoE ^{-/-} control	ApoE ^{-/-} cholesterol
Vitamin C	69.6 ± 8.5 ^a	96.3 ± 3.5 ^b	115 ± 6 ^b	146 ± 5 ^c

The values were mean ± SE for five C57BL/6J and six apoE^{-/-} mice. Differences between group means were considered significant at $P < 0.05$ using Fisher's protected least significant difference test (PLSD). Values with different superscript letters show significant differences at $P < 0.05$

In the present study, we investigated the effects of dietary cholesterol on ceramide and oxidative products of apoB in apoE^{-/-} mice, of which the plasma and aorta responded sufficiently to cholesterol-enriched diets. Our recent study demonstrated that the correlation coefficient between plasma cholesterol and total ceramide in human subjects was particularly high among lipid markers associated with atherosclerosis [11]. Treatment with myriocin, which is a potent and specific SPT inhibitor and is known to have an immunosuppressive activity [29], significantly lowered plasma cholesterol levels of apoE^{-/-} mice in a dose-dependent manner [30]. In this study, we demonstrated that a cholesterol-enriched diet did not affect ceramide levels of the tissues in the wild type mice. However, in apoE^{-/-} mice, the plasma levels of several ceramides in the cholesterol group were significantly

higher than those in the control group and the plasma level of total ceramides in the cholesterol group also tended to be higher than for mice fed a control diet. This result indicated a correlation between increased cholesterol intake and the elevation of the plasma levels of ceramide.

In the liver, the total ceramides of apoE^{-/-} mice were higher than those of the wild control group. However, the difference of ceramides levels between the wild type and the apoE^{-/-} mice in the liver was not so large as that in plasma. In plasma, the difference of total ceramides between the wild type and the apoE^{-/-} mice coincided with the change of cholesterol. Furthermore, the cholesterol-enriched diet did not cause a significant increase in liver ceramide levels. Therefore, a relationship between cholesterol accumulation and ceramide metabolism change in the liver was not supported.

It is well known that a fat-enriched diet is an important factor in the development of atherosclerosis. Overnutrition leads to hypertrophy of adipocytes, and high-fat diets promote obesity [31]. The islet obese fa/fa Zucker diabetic fatty rats exhibit an increase in de novo synthesis of [³H]-ceramide from [³H]-palmitate [32]. Based on these reports, a correlation between ceramide and deposition of visceral fat is suggested. In this study, although the weight of total white adipose tissues in the apoE^{-/-} control group was higher than in the other groups, ceramide levels in the white adipose tissue of the apoE^{-/-} control group were not higher than those of other groups. Therefore, it is suggested that fat accumulation in the white adipose tissue did not increase ceramide content.

Oxidative modification of LDL and its recognition by macrophages have been suggested as being an initial event of atherosclerosis [17]. In this study, we analyzed the oxidation profile of apoB, namely the sum of fragmented and conjugated apoB proteins determined by an immunoblot assay. We reported that these oxidation products of apoB-100, termed B-ox are a reliable indicator of atherosclerosis [15]. In human plasma, the conjugated apoB-100 was higher than the fragmented apoB-100. However, conjugated apoB-100 was not detected clearly in apoE^{-/-} mice. In addition, in plasma of apoE^{-/-} mice it was reported that the major apoB is apoB-48 and the minor apoB is apoB-100 [33]. In this study, conjugated and fragmented apoB-48 were not detected in apoE^{-/-} mice. It is necessary to examine the difference of apoB-100 oxidation between human and mice and the difference of oxidation between apoB-100 and apoB-48.

Our previous studies demonstrated that the reactivity of apoB toward radicals is extremely high and even comparable to vitamin E [14]. Hence degraded apoB fragments were present in normal human plasma and tended to increase with aging [15]. In this study, the apoE^{-/-} chole-

sterol group, which demonstrated a significant increase in the size of lesions as is well established [33], also exhibited decreased apoB and increased fragmented apoB proteins compared to the control group. These results demonstrated that the cholesterol diet increased the development of atherosclerotic lesions and promoted oxidation of apoB in the apoE^{-/-} mice. We reported that cross-linked and fragmented apoB-100 is a reliable index of atherosclerosis and oxidative stress [15]. Therefore, it is suggested that fragmentation of apoB is also a reliable indicator of atherosclerosis in apoE^{-/-} mice as well as humans.

OxLDL have been shown to induce apoptosis of culture cells [34, 35]. Ceramides also have been shown to cause apoptosis in a variety of cells. Apoptosis of endothelial cells is widely implicated in the early stage of atherosclerosis. It was reported that oxLDL was involved in the formation of various sphingolipid mediators [36] and activated the generation of ceramide in endothelial cells [37]. Our results also demonstrated that apoE^{-/-} mice, which showed increased size of lesions, exhibited higher ceramide levels and fragmented apoB in plasma. Based on these results, a correlation between increased oxLDL and ceramide is suggested. However, oxLDL-induced activation of the SMase-ceramide pathway has not yet been fully studied and is still controversial. Further studies are needed to clarify the relationship between LDL oxidation and ceramide metabolism.

Vitamin C is a potent water-soluble antioxidant that scavenges reactive oxygen species [38, 39]. Sublethal lipopolysaccharide, which is associated with oxidative stress, temporarily increased liver vitamin C in the mouse [40]. In addition, the deficiency of glutathione, which plays various important roles in the protection against oxidant stress [41], increased hepatic ascorbate synthesis in mice [42]. These studies indicate that vitamin C synthesis is enhanced by oxidative stress in mice. In this study, plasma vitamin C in apoE^{-/-} mice was higher than that in the wild type mice. It is suggested that apoE^{-/-} mice at this young age increased vitamin C production compared to the wild type mice to prevent increased oxidative stress. In addition, plasma vitamin C in the wild type and apoE^{-/-} mice fed a cholesterol diet was higher than in those fed a control diet. The increase of B-ox in the apoE^{-/-} mice fed a cholesterol diet suggested enhanced stress, which resulted in the elevation of plasma vitamin C just like in the mice under enhanced oxidative stress as described above [40, 42].

In conclusion, this study demonstrated that dietary cholesterol increased ceramide levels and products of oxidized LDL in plasma of the apoE^{-/-} mice. In addition, we propose that ceramides, the toxicities of which are much higher than that of cholesterol, are a new risk factor for atherosclerosis.

Acknowledgments This work was supported by the Ministry of Education, Culture, Sports, Science, and Technology of Japan, and the Uehara Memorial Foundation.

Reference

- Hannun YA, Obeid LM (2002) The ceramide-centric universe of lipid-mediated cell regulation: stress encounters of the lipid kind. *J Biol Chem* 277:25847–25850
- Merrill AH (2002) De novo sphingolipid biosynthesis: a necessary, but dangerous, pathway. *J Biol Chem* 277:25843–25846
- Olivera A, Spiegel S (2001) Sphingosine kinase: a mediator of vital cellular functions. *Prostaglandins Other Lipid Mediat* 64:123–134
- Kolesnick R (1992) Ceramide: a novel second messenger. *Trends Cell Biol* 2:232–236
- Merrill AH, Jones DD (1990) An update of the enzymology and regulation of sphingomyelin metabolism. *Biochim Biophys Acta* 1044:1–12
- Jiang XC, Paultre F, Pearson TA, Reed RG, Francis CK, Lin M, Berglund L, Tall AR (2000) Plasma sphingomyelin level as a risk factor for coronary artery disease. *Arterioscler Thromb Vasc Biol* 20:2614–2618
- Noel C, Marcel YL, Davignon J (1972) plasma phospholipids in the different types of primary hyperlipoproteinemia. *J Lab Clin Med* 79:611–612
- Nelson JC, Jiang XC, Tabas I, Tall A, Shea S (2006) Plasma sphingomyelin and subclinical atherosclerosis: findings from the multi-ethnic study of atherosclerosis. *Am J Epidemiol* 163:903–912
- Park TS, Panek RL, Mueller SB, Hanselman JC, Rosebury WS, Robertson AW, Kindt EK, Homan R, Karathanasis SK, Reckter MD (2004) Inhibition of sphingomyelin synthesis reduces atherogenesis in apolipoprotein E-knockout mice. *Circulation* 110:3465–3471
- Hojjati MR, Li Z, Zhou H, Tang S, Huan C, Ooi E, Lu S, Jiang XC (2005) Effect of myriocin on plasma sphingolipid metabolism and atherosclerosis in ApoE-deficient mice. *J Biol Chem* 280:10284–10289
- Ichi I, Nakahara K, Miyashita Y, Hidaka A, Kutsukake S, Inoue K, Maruyama T, Miwa Y, Harada-Shiba M, Tsushima M, Kojo S (2006) Association of ceramides in human plasma with risk factors of atherosclerosis. *Lipids* 41:859–863
- Steinberg D, Parthasarathy S, Carew TE, Khoo JC, Witztum JL (1989) Beyond cholesterol: modifications of low density lipoprotein that increase its atherogenicity. *N Engl J Med* 320:915–924
- Witztum JL, Steinberg D (1991) Role of oxidized low density lipoprotein in atherogenesis. *J Clin Invest* 88:1785–1792
- Hashimoto R, Narita S, Yamada Y, Tanaka K, Kojo S (2000) Unusually high reactivity of apolipoprotein B-100 among proteins to radical reactions induced in human plasma. *Biochem Biophys Acta* 1483:236–240
- Hashimoto R, Matsukawa N, Nariyama Y, Ogiri Y, Hamagawa E, Tanaka K, Usui Y, Nakano S, Maruyama T, Kyotani S, Tsushima M, Kojo S (2002) Evaluation of apolipoprotein B-100 fragmentation and cross-link in the serum as an index of atherosclerosis. *Biochim Biophys Acta* 1584:123–128
- Pentikainen MO, Lehtonen EMP, Kovanen PT (1996) Aggregation and fusion of modified low density lipoprotein. *J Lipid Res* 37:2638–2649
- Ross R (1993) The pathogenesis of atherosclerosis: a perspective for 1990s. *Nature* 362:801–809
- Schissel SL, Tweedie-Hardman J, Rapp JH, Graham G, Williams KJ, Tabas I (1996) Rabbit aorta and human atherosclerotic lesions hydrolyze the sphingomyelin of retained low-density lipoprotein. *J Clin Invest* 98:1455–1464
- Xu XX, Tabas I (1991) Sphingomyelinase enhances low density lipoprotein uptake and ability to induce cholesteryl ester accumulation in macrophages. *J Biol Chem* 266:24849–24858
- Williams RD, Sgoutas DS, Zaatari GS (1986) Enzymology of long-chain base synthesis by aorta: induction of serine palmitoyltransferase activity in rabbit aorta during atherogenesis. *J Lipid Res* 27:763–770
- Zhang SH, Reddick RL, Piedrahita JA, Maeda N (1992) Spontaneous hypercholesterolemia and arterial lesions in mice lacking apolipoprotein E. *Science* 258:468–471
- Ikeda I, Tanaka K, Sugano M, Vahouny GV, Gallo LL (1988) Discrimination between cholesterol and sitosterol for absorption in rats. *J Lipid Res* 29:1583–1591
- Fletcher MJ (1968) A colorimetric method for estimation of serum triglycerides. *Clin Chim Acta* 22:393–397
- Kishida E, Nishimoto Y, Kojo S (1992) Specific determination of ascorbic acid with chemical derivatization and high-performance liquid chromatography. *Anal Chem* 64:1505–1507
- Folch J, Ascoli I, Lees M, Meath JA, LeBaron N (1966) Preparation of lipid extracts from brain tissues. *J Biol Chem* 191:833–841
- Yamada Y, Kajiwara K, Yano M, Kishida E, Masuzawa Y, Kojo S (2001) Increase of ceramides and its inhibition by catalase during chemically induced apoptosis of HL-60 cells determined by electrospray ionization tandem mass spectrometry. *Biochim Biophys Acta* 1532:115–120
- Huwyler A, Kolter T, Pfeilschifter J, Sandhoff K (2000) Physiology and pathophysiology of sphingolipid metabolism and signaling. *Biochim Biophys Acta* 1485:63–99
- Levade T, Auge N, Veldman RJ, Cuvillier O, Negre-Salvayre A, Salvayre R (2001) Sphingolipid mediators in cardiovascular cell Biology and pathology. *Circ Res* 89:957–968
- Miyake Y, Kozutsumi Y, Nakamura S, Fujita T, Kawasaki T (1995) Serine palmitoyltransferase is the primary target of a sphingosine-like immunosuppressant, ISP-1/myriocin. *Biochem Biophys Res Commun* 211:396–403
- Park TS, Panek RL, Reckter MD, Mueller SB, Rosebury WS, Robertson A, Hanselman JC, Kindt E, Homan R, Karathanasis SK (2006) Modulation of lipoprotein metabolism by inhibition of sphingomyelin synthesis in ApoE knockout mice. *Atherosclerosis* 189:264–272
- Golay A, Bobbioni E (1997) The role of dietary fat in obesity. *Int J Obes Relat Metab Disord* 21:2–11
- Shimabukuro M, Higa M, Zhou YT, Wang MY, Newgard CB, Unger RH (1998) Lipoapoptosis in beta-cells of obese prediabetic fa/fa rats. Role of serine palmitoyl transferase overexpression. *J Biol Chem* 273:32487–32490
- Ishibashi S, Herz J, Maeda N, Goldstein JL, Brown MS (1994) The two-receptor model of lipoprotein clearance: tests of the hypothesis in “knockout” mice lacking the low density lipoprotein receptor, apolipoprotein E, or both proteins. *Proc Natl Acad Sci USA* 91: 4431–4435
- Escargueil I, Nègre-Salvayre A, Pieraggi MT, Salvayre R (1992) Oxidized low density lipoproteins elicit DNA fragmentation of cultured lymphoblastoid cells. *FEBS Lett* 305:155–159
- Harada-Shiba M, Kinoshita M, Kamido H, Shimokado K (1998) Oxidized low density lipoprotein induces apoptosis in cultured human umbilical vein endothelial cells by common and unique mechanisms. *J Biol Chem* 273:9681–9687
- Chatterjee S (1998) Sphingolipids in atherosclerosis and vascular biology. *Arterioscler Thromb Vasc Biol* 18:1523–1533
- Auge N, Andrieu N, Negre-Salvayre A, Thiers JC, Levade T, Salvayre R (1996) The sphingomyelin-ceramide signaling pathway is involved in oxidized low density lipoprotein-induced cell proliferation. *J Biol Chem* 271:19251–19255

38. Frei B, England L, Ames BN (1989) Ascorbate is an outstanding antioxidant in human blood plasma. *Proc Natl Acad Sci USA* 86:6377–6381
39. Kojo S (2004) Vitamin C, basic metabolism and its function as an index of oxidative stress. *Curr Med Chem* 11:1041–1064
40. Kuo SM, Tan CH, Dragan M, Wilson JX (2005) Endotoxin increases ascorbate recycling and concentration in mouse liver. *J Nutr* 135:2411–2416
41. Rahman I, MacNee W (2000) Oxidative stress and regulation of glutathione synthesis in lung inflammation. *Eur Respir J* 16:16534–16554
42. Martensson J, Meister A (1992) Glutathione deficiency increases hepatic ascorbic acid synthesis in adult mice. *Proc Natl Acad Sci USA* 89:11566–11568



Gene delivery with biocompatible cationic polymer: Pharmacogenomic analysis on cell bioactivity

Kayo Masago^{a,1}, Keiji Itaka^{a,1}, Nobuhiro Nishiyama^a,
Ung-il Chung^{a,c,d}, Kazunori Kataoka^{a,b,d,*}

^aDivision of Clinical Biotechnology, Center for Disease Biology and Integrative Medicine, Graduate School of Medicine, The University of Tokyo, Japan

^bDepartment of Materials Science and Engineering, Graduate School of Engineering, The University of Tokyo, Japan

^cDepartment of Bioengineering, Graduate School of Engineering, The University of Tokyo, Japan

^dCenter for Nanobio Integration, The University of Tokyo, 7-3-1 Hongo, Bunkyo-ku, Tokyo 113-0033, Japan

Received 7 June 2007; accepted 10 July 2007

Available online 30 July 2007

Abstract

The availability of non-viral gene delivery systems is determined by their capacity and safety during gene introduction. In this study, the safety issues of polyplex were analyzed from the standpoint of the biomolecular mechanisms. P[Asp(DET)], a newly developed polymer, polyasparagine carrying the *N*-(2-aminoethyl)aminoethyl group as the side chain which was recently revealed to show good transfection efficiency to primary cells, was compared to conventional linear poly(ethylenimine) (LPEI). After transfection toward a bioluminescent cell line, P[Asp(DET)] maintained the expression level of stably expressing luciferase. In contrast, LPEI showed a decrease in the luciferase expression, while the similar expression of exogenous reporter gene was obtained. Evaluation of the housekeeping genes expression as well as the profiles of pDNA uptake after transfection suggested the time-dependent toxicity of LPEI that perturbs cellular homeostasis. Consistently, the induction of osteogenic differentiation by functional gene introduction was achieved only by P[Asp(DET)], even though appreciable expression of the gene was achieved by LPEI. It is crucial that this aspect of safety be taken into account, especially when the gene introduction is applied to primary cells to regulate such cell function as differentiation. This biomolecular analysis focusing on cellular homeostasis is beneficial for assessing the practicability of the gene delivery systems for clinical application.

© 2007 Elsevier Ltd. All rights reserved.

Keywords: Biocompatibility; Gene transfer; Cationic polymer; Cytotoxicity; Cell differentiation

1. Introduction

Gene therapies have attracted progressive attention for the treatment of numerous intractable diseases, but the lack of safe and efficient gene-delivery systems is an obstacle to their clinical application. Viral vectors are known to be highly potent gene delivery systems, yet may also induce adverse side effects, including severe immunological and toxicological responses. In fact, recent clinical

trials using viral vectors have been halted due to unprecedented toxicity, including the death of a patient [1–4]. Therefore, non-viral gene carriers such as cationic lipids and polymers are expected to be an alternative to viral vectors directing therapeutic genes to target tissues.

The availability of gene carriers is largely determined by their transfection efficiency and cytotoxicity. Although the latter is generally evaluated through the viability assay of cultured cells such as an MTT assay [5], an MTT assay only reflects the non-specific outcome of cell death. Synthetic carriers may induce side effects including complement activation, carcinogenicity, teratogenicity and immunogenicity, all of which are serious concerns for clinical application [6]. Thus, the safety issues of non-viral gene carriers, both on a cellular and systemic basis,

*Corresponding author. Department of Materials Engineering, Graduate School of Engineering, The University of Tokyo, 7-3-1 Hongo, Bunkyo-ku, Tokyo 113-0033, Japan. Tel.: +81 3 5841 7138; fax: +81 3 5841 7139.

E-mail address: kataoka@bmw.t.u-tokyo.ac.jp (K. Kataoka).

¹These authors contributed equally to this work.

are critical for their clinical development, requiring careful analysis of the toxicity by exploring the biomolecular mechanisms. In this regard, a pharmacogenomic analysis of the global gene expression in the transfected cells is of particular interest. This approach has recently been advocated as polymer genomics or material genomics, and several studies have been reported to have applied it for the evaluation of non-viral gene carriers [7,8].

Recently, we developed a novel block cationer-based gene delivery system that showed excellent capacity for *in vitro* transfection to primary cells [9]. This system is composed of plasmid DNA (pDNA) and poly(ethylene glycol)-block-polyasparagine carrying the *N*-(2-aminoethyl) aminoethyl group $(\text{CH}_2)_2\text{NH}(\text{CH}_2)_2\text{NH}_2$ as the side chain (PEG-PAsp[DET]). Ethylene diamine units located at the side chain are only half protonated under neutral pH and are thus feasible candidates to perform the so-called proton sponge effect, which has been believed to be the major mechanism for the excellent transfection efficiency of some polyamine derivatives having substantially lowered pKa such as poly(ethylenimine) (PEI) [10–12]. As well as the good transfection efficiency, the polyplex micelles from this block cationer showed minimal cytotoxicity toward various primary cells, achieving the successful *in vivo* gene introduction to the vascular lesions [13] and the effective induction of cell differentiation both *in vitro* and *in vivo* through the effective expression of the genes encoding transcriptional factors [14].

These results motivated us to perform an additional toxicogenomic study of P[Asp(DET)] in order to ensure the safety for future clinical application. Linear PEI (LPEI) was used as a control, representing the common polycation for the construction of polyplexes. Although P[Asp(DET)] and LPEI both have a buffering capacity under an endosomal pH, they showed a considerable difference in the toxicological profiles which revealed the appreciably lowered toxicity of the former compared to the latter. In particular, the time-dependent change in the pharmacogenomic toxicity toward the targeted cells was evaluated in detail, in regards to the capacity of inducing cell differentiation through the transfection of functional genes encoded in the encapsulated pDNA in the polyplex.

2. Materials and methods

2.1. Materials

pGL3-control pDNA encoding firefly luciferase (Promega, Madison, WI, USA), pRL-CMV pDNA encoding renilla luciferase (RL) (Promega), and EGFP-C1 pDNA encoding EGFP (Clontech, Palo Alto, CA, USA) were amplified in the *Escherichia coli* strain DH5 α , which was isolated and purified using a QIAGEN HiSpeed Plasmid Maxi Kit (Qiagen, Hilden, Germany). pCMV5 pDNA expressing HA-tagged mouse caALK6 and pcDEF3 pDNA expressing Flag-tagged mouse Runx2 were generous gifts from Dr. M. Krüppel (Mt. Sinai Hospital, Toronto, ON, Canada) and Dr. K. Miyazono (University of Tokyo, Tokyo, Japan), respectively. The concentration of DNA was determined by measuring the UV absorption at 260 nm.

2.2. Cells

HuH-7 cells were obtained from the Riken Cell Bank (Tsukuba, Japan). Bioluminescent cells (HuH-7-luc) stably expressing firefly luciferase were kindly provided by Mr. S. Matsumoto (University of Tokyo). Dulbecco's modified Eagle's medium (DMEM) and fetal bovine serum (FBS) were purchased from Sigma-Aldrich (St. Louis, MO, USA).

2.3. Polycations for the preparation of polyplex

LPEI (Exgen 500, $M_w = 22$ kDa) was purchased from MBI Fermentas (Burlington, ON, Canada). Diethylenetriamine (DET) was purchased from Tokyo Kasei Kogyo (Tokyo, Japan). All other chemicals were purchased from Wako Pure Chemical Industries (Osaka, Japan). P[Asp(DET)] was synthesized by the side-chain aminolysis reaction of the poly(β -benzyl L-aspartate) (PBLA) as previously reported [9]. Briefly, the PBLA was synthesized by the ring-opening polymerization of the β -benzyl-L-aspartate *N*-carboxyanhydride (BLA-NCA) initiated by the primary amine of *n*-butylamine in *N,N*-dimethylformamide (DMF)/dichloromethane (1:10) at 40 °C, followed by the acetylation of the *N*-terminal amine with acetic anhydride. Gel permeation chromatography (GPC) was performed to confirm a unimodal molecular weight distribution (M_w/M_n 1.20) of PBLA by TOSHO HLC-8220 (columns: TSK-gel G4000HHR + G3000HHR, eluent: DMF + 10 mM LiCl, $T = 40$ °C, detector: refractive index). The degree of polymerization of PBLA was determined as 98 from the ^1H NMR spectrum (JEOL EX300 spectrometer: JEOL, Tokyo, Japan). Then, the side-chain aminolysis reaction of PBLA was performed by mixing the DMF solution of PBLA (50 mg/ml) with a 50-fold excess of DET in DMF at 40 °C to obtain P[Asp(DET)].

2.4. Polyplex formation

Each polyplex sample with a pDNA concentration of 33 $\mu\text{g}/\text{mL}$ was prepared by simply mixing pDNA and polycation (LPEI or P[Asp(DET)]) at the indicated *N/P* ratio ($=$ [total amines in polycation]/[DNA phosphates]) in a 10 mM Tris-HCl (pH 7.4) buffer solution.

2.5. Dual luciferase measurement on HuH-7-luc cells transfected with pRL-CMV pDNA

HuH-7-luc cells were seeded on 96-well culture plates (3×10^3 cells/well) and incubated overnight in 100 μl DMEM supplemented with 10% FBS and penicillin/streptomycin. After the culture medium was replaced with fresh medium containing 10% FBS, 5.5 μl of the polyplexes composed of P[Asp(DET)] or LPEI (final DNA concentration: 33 $\mu\text{g}/\text{ml}$) were applied to each well. After 24 h, the medium was changed to remove the polyplexes, followed by further incubation for 24 or 48 h. The firefly and RL activities were measured using a Dual-Luciferase Reporter Assay System (Promega) according to the protocol provided by the manufacturer, using a GloMaxTM 96 Microplate Luminometer (Promega).

2.6. Cell proliferation assay

HuH-7-luc cells (6×10^4 cells/well) were seeded in six-well plates and cultured overnight. After the transfection as described above (polyplex solution: 90 $\mu\text{l}/\text{well}$), the cells were washed with phosphate-buffered saline (PBS), trypsinized, and scraped off. Then the cell number was counted by a nucle counter (Chemometec, Tokyo, JAPAN) following the protocol provided by the manufacturer. The measurement was duplicated.

2.7. Lactate dehydrogenase (LDH) assay

The degree of membrane destabilization was examined by lactate dehydrogenase (LDH) activity liberated from the cytoplasm. The cells were plated on 96-well plates and incubated overnight in 100 μl of DMEM